2nd IFAC Workshop on Automatic Control in Offshore Oil and Gas Production,
May 27-29, 2015, Florianópolis, Brazil

Estimation of Flow Rate and Viscosity in a Well with an Electric Submersible Pump using Moving Horizon Estimation ⋆

Benjamin J.T. Binder * **Alexey Pavlov** ** **Tor A. Johansen** ***

* *Department of Engineering Cybernetics, Norwegian University of Science and Technology, O.S. Bragstads plass 2D, NO-7491 Trondheim, Norway (e-mail: benjamin.binder@itk.ntnu.no).*
** *Statoil ASA Research and Development Center, P.b. 1004, NO-3905 Porsgrunn, Norway (e-mail: alepav@statoil.com)*
*** *Center for Autonomous Marine Operations and Systems (AMOS), Department of Engineering Cybernetics, Norwegian University of Science and Technology, O.S. Bragstads plass 2D, NO-7491 Trondheim, Norway (e-mail: tor.arne.johansen@itk.ntnu.no).*

Abstract: A Moving Horizon Estimator (MHE) is designed for a petroleum production well with an Electric Submersible Pump (ESP) installed for artificial lift. The focus is on estimating the flow rate from the well, the viscosity of the produced fluid, and the productivity index of the well. The software package ACADO is used to implement a Moving Horizon Estimator using a third-order nonlinear model. Simulation results show that the implemented estimator is able to estimate the desired variable and parameters. The resulting C-code solver is very fast, admitting real-time implementation.

Keywords: Petroleum Production, Electric Submersible Pumps, Estimators, Moving Horizon Estimation, Flow Rate Allocation, Production Optimization

1. INTRODUCTION

Information about the flow rate and phase fractions from individual wells in an oil field is important for flow rate allocation and production optimization. Measurements of these have traditionally been performed with specialized and costly instrumentation. Multi-phase flow metering has been a challenge for offshore applications, both due to the complexity of such fields, and space requirements, costs and uncertainties associated with such instrumentation (Varón et al., 2013). Moreover, for fields producing oil with a high viscosity, multi-phase flow meters may not be very reliable.

The Electric Submersible Pump (ESP) is one of the most widely used methods for artificial lift in the oil industry (Takacs, 2009; Varón et al., 2013). There are a number of variables that affect the life-time of ESP installations, such as power consumption, flow rate, pressure, temperature, thrust forces and vibration. Operation outside of certain limits on these variables may lead to failure or reduced life-time of the ESP, which has a huge economic impact, both due to the costs of replacing the pump, and the loss of production.

Reliable measurements are difficult to obtain for many important variables and parameters in ESP-lifted wells. As a lot of instrumentation is usually included in ESP installations, using the ESP as a flow meter has recently been investigated. Extensive testing of both flow meters and ESPs for flow allocation purposes was performed in Beall et al. (2011). It was shown that flow meter accuracy is highly dependent on correct fluid characterization, specifically viscosity and phase fractions are important parameters. In Olsen et al. (2012) the ESP tests and flow rate allocation was further discussed, and the results from the ESP tests were used to develop an algorithm that estimates flow rates based on measurements from the ESP system and fluid properties, combined with models of the ESP system components. The flow rate measurements depend on the pump speed, ESP head or brake horsepower, and the viscosity of the fluid. Promising results with this approach were reported. Uncertainties in the flow rate measurements by using the ESP as a flow meter were investigated in Varón et al. (2013), where it was shown that this depends on the pump speed and fluid viscosity. This reveals that a main limitations in this approach is that it depends heavily on correct information about certain parameters, such as the viscosity of the produced fluid.

Estimators (observers) are usually implemented to estimate unmeasured states in a system model that is used for control and monitoring purposes. The Kalman Filter is an efficient solution to the estimation problem for linear systems, but the estimation of nonlinear systems is still a challenging problem. Various nonlinear extensions of the linear Kalman filter has been developed, including the Extended Kalman Filter (EKF) and the Unscented Kalman

⋆ This work is funded by the Research Council of Norway and Statoil through the PETROMAKS project No. 215684: Enabling High-Performance Safety-Critical Offshore and Subsea Automatic Control Systems Using Embedded Optimization (emOpt)

Copyright © 2015, IFAC

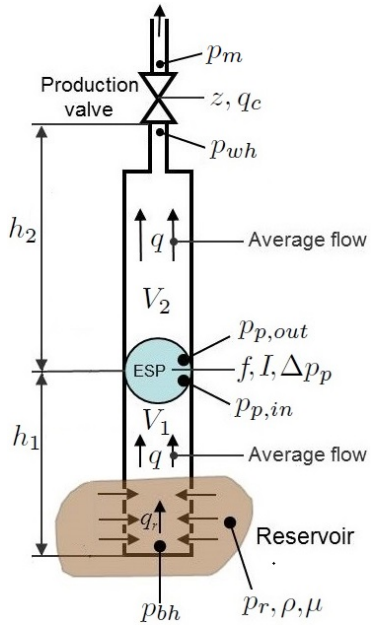

Fig. 1. ESP-lifted well

Filter (UKF), the EKF probably being the most commonly implemented estimator for nonlinear systems (Julier and Uhlmann, 2004). The Moving Horizon Estimator (MHE) (Rao et al., 2003) is an optimization-based method for nonlinear estimation that works on a limited number of past measurements (a 'window' or 'horizon'). The main advantages of MHE is the explicit consideration of state and parameter constraints, optimality of the estimates (in a least-squares sense), and the stability properties (Kühl et al., 2011).

In the recent years, several researchers have investigated estimation in petroleum wells based on dynamic models of the wells. Estimation in gas-lifted wells was investigated e.g. in Bloemen et al. (2004); Eikrem et al. (2004); Aamo et al. (2005), and for drilling applications in e.g. Siahaan and Nygaard (2008); Paasche et al. (2011); Kaasa et al. (2012); Nikoofard et al. (2014); Hasan and Imsland (2014).

In this paper, MHE is implemented for a well with an ESP and a production choke valve, as shown in Fig. 1. The focus is on estimating the flow q from the well, the viscosity μ of the produced fluid, and the productivity index PI of the well, based on measurements that typically are available in such systems. Both flow rate of the produced fluid and the well productivity index (PI) are very important parameters for flow rate allocation and production optimization, and both flow rate and viscosity of the produced fluid are needed to determine whether the ESP has safe operating conditions.

A main feature of the approach presented in this paper is that not only a model of the ESP, but a dynamic model of the entire well is used to get better estimates of the unknown parameters. This includes models of the pressure drop in the well between the ESP and the production choke, the pressure drop over the production choke, and the inflow from the reservoir. Moreover, the estimations are based on measurements from a certain time window (estimation horizon), which adds up to reliability and accuracy of the estimates.

Table 1. Model variables

Inputs		**Unit**	**Meas**
f	ESP frequency	Hz	yes
z	Production choke valve opening	-	yes
Pressures		**Unit**	**Meas**
p_m	Manifold pressure	Pa	yes
p_{wh}	Wellhead pressure	Pa	yes
$p_{p,out}$	ESP outlet pressure	Pa	yes
$p_{p,in}$	ESP inlet pressure	Pa	yes
Δp_p	Pressure difference across ESP	Pa	yes
p_{bh}	Bottomhole pressure in well	Pa	no
Δp_f	Frictional pressure drop in the well	Pa	no
F_1	Frictional pressure drop below ESP	Pa	no
F_2	Frictional pressure drop above ESP	Pa	no
Flow rates		**Unit**	**Meas**
q	Average flow rate in well	m^3/s	no
q_c	Flow rate through production choke	m^3/s	no
q_r	Inflow from reservoir into well	m^3/s	no
ESP		**Unit**	**Meas**
I	Electric current in ESP motor	A	yes
H	Head developed by ESP	m	no
P	ESP brake horsepower (BHP)	W	no

2. SYSTEM MODEL

The estimation in this paper is based on a dynamic model of the well and the ESP. The estimation also depends on available system information, such as measured variables, known model parameters and empirical test data. In this section, the model that is used in the estimator is presented, and the information assumed to be available is outlined.

2.1 Model Variables

The considered well is shown in Fig. 1. (A vertical well is depicted, but the model also describes deviated wells.) These are the main variables in the system:

- The control inputs to the system are the rotational frequency f of the ESP, and the production choke valve opening denoted z.
- p_m denotes the manifold pressure, which is treated as a disturbance in the model.
- The wellhead pressure is denoted p_{wh}, and the bottomhole pressure is denoted p_{bh}.
- $p_{p,in}$ and $p_{p,out}$ denote the pressures at the inlet and outlet of the ESP, and $\Delta p_p = p_{p,out} - p_{p,in}$ the pressure increase provided by the ESP.
- I denotes the electric current supplied to the ESP motor.
- q denotes the average flow rate in the well, q_c the flow rate through the production choke valve, and q_r the inflow from the reservoir.

A complete list of variables that are used in the model is given in table 1. Model parameters are described in sections 2.4 and 2.5.

2.2 Measurements

The following assumptions are made regarding available measurements in the system:

Copyright © 2015, IFAC

- Pressure sensors are installed at the production manifold, so that the manifold pressure p_m and the wellhead pressure p_{wh} are measured.
- The ESP is equipped with pressure sensors so that $p_{p,in}$, $p_{p,out}$ and thus Δp_p are measured.
- The Variable Speed Drive (VSD) provides measurements of the electric current I supplied to the ESP motor, and the rotational frequency f of the ESP. [1]
- The choke opening z is known or measured.

The variables that are assumed to be measured are also indicated in table 1.

2.3 Model

The model used in the estimator is based on a simple model of an ESP-lifted well developed by Statoil (Pavlov and Alstad, 2010; Pavlov et al., 2014), and is modified to include Viscosity Correction Factors (VCFs) in the model of the ESP. The resulting model is a nonlinear third-order model, given by the following differential equations:

$$\dot{p}_{bh} = \frac{\beta_1}{V_1}(q_r - q) \tag{1a}$$

$$\dot{p}_{wh} = \frac{\beta_2}{V_2}(q - q_c) \tag{1b}$$

$$\dot{q} = \frac{1}{M}(p_{bh} - p_{wh} - \rho g h_w - \Delta p_f + \Delta p_p) \tag{1c}$$

and the following algebraic equations:

Flow:
$$q_r = \mathrm{PI}\,(p_r - p_{bh}) \tag{2a}$$

$$q_c = C_c\sqrt{p_{wh} - p_m}\,z \tag{2b}$$

Friction:
$$\Delta p_f = F_1 + F_2 \tag{2c}$$

$$F_i = 0.158 \cdot \frac{\rho L_i q^2}{D_i A_i^2}\left(\frac{\mu}{\rho D_i q}\right)^{\frac{1}{4}} \tag{2d}$$

ESP:
$$\Delta p_p = \rho g H \tag{2e}$$

$$H = C_H(\mu)H_0(q_0)\left(\frac{f}{f_0}\right)^2 \tag{2f}$$

$$q_0 = \frac{q}{C_q(\mu)}\left(\frac{f_0}{f}\right) \tag{2g}$$

Additional measurements are given by the following equations:

$$I = \frac{I_{np}}{P_{np}}P \tag{3a}$$

$$P = C_P(\mu)P_0(q_0)\left(\frac{f}{f_0}\right)^3 \tag{3b}$$

$$p_{p,in} = p_{bh} - \rho g h_1 - F_1 \tag{3c}$$

Depending on the fluid properties and pressure/temperature conditions in the well, density and viscosity may be different in different parts of the well. In this paper we consider a well where changes in these properties throughout the well are not significant. This corresponds to a well producing with a low gas-to-oil ratio and primarily with oil continuous flow.

[1] In most cases an ESP is driven by an asynchronous motor. This means that the rotational frequency f of the ESP shaft will be different from the frequency of the AC current supplied to the motor. Many modern VSDs for ESPs can provide accurate estimates of the shaft speed, and the assumption that f is measured will be valid for such VSDs.

Table 2. Model parameters

Well dimensions and other known constants			
g	Gravitational acceleration constant	9.81	m/s^2
C_c	Choke valve constant	$2{\cdot}10^{-5}$	*
A_1	Cross-section area of pipe below ESP	0.008107	m^2
A_2	Cross-section area of pipe above ESP	0.008107	m^2
D_1	Pipe diameter below ESP	0.1016	m
D_2	Pipe diameter above ESP	0.1016	m
h_1	Height from reservoir to ESP	200	m
h_w	Total vertical distance in well	1 000	m
L_1	Length from reservoir to ESP	500	m
L_2	Length from ESP to choke	1 200	m
V_1	Pipe volume below ESP	4.054	m^3
V_2	Pipe volume above ESP	9.729	m^3
ESP data			
f_0	ESP characteristics reference freq.	60	Hz
I_{np}	ESP motor nameplate current	65	A
P_{np}	ESP motor nameplate power	$1.625{\cdot}10^5$	W
Parameters from fluid analysis and well tests			
β_1	Bulk modulus below ESP	$1.5{\cdot}10^9$	Pa
β_2	Bulk modulus above ESP	$1.5{\cdot}10^9$	Pa
M	Fluid inertia parameter	$1.992{\cdot}10^8$	kg/m^4
ρ	Density of produced fluid	950	kg/m^3
p_r	Reservoir pressure	$1.26{\cdot}10^7$	Pa
Unknown parameters			
PI	Well productivity index	$2.32{\cdot}10^{-9}$	$m^3/s/Pa$
μ	Viscosity of produced fluid	Varying	$Pa \cdot s$

* Appropriate SI units

2.4 Model Parameters

An overview of the parameters used in the model is given in table 2. This includes fixed parameters (such as physical dimensions of the well and the ESP motor ratings) and parameters assumed to be obtained from analysis of fluid samples (such as density ρ, bulk moduli β_i, and the fluid inertia parameter M). The reservoir pressure p_r is also assumed to be known from dedicated well tests. The well productivity index PI and the fluid viscosity μ are unknown parameters (to be estimated).

2.5 ESP Characteristics and Viscosity Correction Factors

ESP characteristics for Head $H_0(q)$ and Brake Horsepower $P_0(q)$, as well as Viscosity Correction Factors (VCFs) $C_q(\mu)$, $C_H(\mu)$ and $C_P(\mu)$ for flow, head and BHP, respectively, are also assumed to be known for the particular ESP used in the well. The ESP characteristics are given for water at a given reference frequency, and are provided by the pump vendor, while VCFs are usually obtained from published sources (HI, 1969), or through dedicated lab tests. The characteristics that are used in the model are stated in table 3.

The ESP characteristics and VCFs used in this paper are given by polynomials on the form:

$$P(x) = \sum_{i=0}^{4} c_i x^i \tag{4}$$

with the corresponding coefficients c_i for each variable given in table 4. The VCFs are also shown in Fig. 2, and are valid for viscosities up to 500 centipoise.

Copyright © 2015, IFAC

Table 3. ESP characteristics and Viscosity Correction Factors (VCFs)

Var.	Description	Unit
H_0	ESP head characteristics	m
P_0	ESP BHP characteristics	W
q_0	Theoretical flow rate at reference freq.	m^3/s
C_H	VCF for head	-
C_P	VCF for brake horsepower of the ESP	-
C_q	VCF for ESP flow rate	-

Table 4. Polynomial coefficients

	c_4	c_3	c_2	c_1	c_0
H_0	0	0	-1.2454e6	7.4959e3	9.5970e2
P_0	0	-2.3599e9	-1.8082e7	4.3346e6	9.4355e4
C_q	2.7944	-6.8104	6.0032	-2.6266	1
C_H	0	0	0	-0.03	1
C_P	-4.4376	11.091	-9.9306	3.9042	1

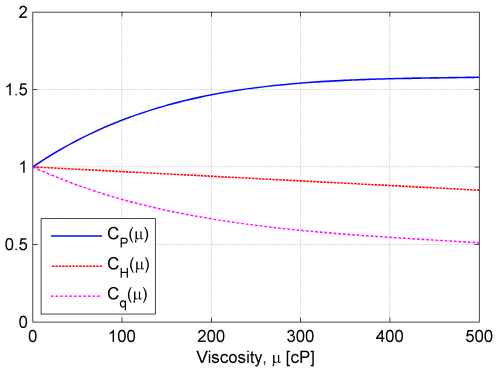

Fig. 2. Viscosity correction factors

3. MOVING HORIZON ESTIMATION

A Moving Horizon Estimator (MHE) is implemented to estimate the flow rate q and the unknown parameters μ and PI. The implementation of the estimator is outlined in this section.

3.1 ACADO Code Generation Tool

The estimator is implemented using the Code Generation tool included in the ACADO toolkit (Automatic Control And Dynamic Optimization toolkit) (Houska et al., 2011). This tool exports highly efficient C-code for solving nonlinear MPC and MHE problems by means of the real-time iteration scheme with Gauss-Newton Hessian approximation (Houska et al., 2009–2013). The solver method is based on results presented in Diehl et al. (2002), and is further described in Kühl et al. (2011). The scheme uses only one iteration per measurement sample, and divides the problem into a preparation phase and a feedback phase. The generated ACADO solver calls an embedded variant of the active-set online QP solver qpOASES, implemented in basic C++.[2] (Houska et al., 2009–2013; Ferreau et al., 2014)

[2] ACADO has an interface that allows for implementation of other QP solvers, but qpOASES is the default solver and was used in this paper.

3.2 MHE Formulation for ACADO Code Generation Tool

The ACADO Code Generation tool can be used to solve an MHE problem formulated as follows:

$$\min_{x,u} \ \|x_0 - x_{AC}\|^2_{S_{AC}} + \sum_{k=0}^{N-1} \|h(x_k, u_k) - \bar{y}_k\|^2_{W_k} + \|h_N(x_N) - \bar{y}_N\|^2_{W_N} \quad (5a)$$

Subject to:

$$x_{k+1} = F(x_k, u_k, d_k), \qquad k = 0, ..., N-1 \quad (5b)$$

$$x_k^{low} \le x_k \le x_k^{high}, \qquad k = 0, ..., N \quad (5c)$$

$$u_k^{low} \le u_k \le u_k^{high}, \qquad k = 0, ..., N-1 \quad (5d)$$

N is the length of the estimation window (number of intervals/samples), the subscript k refers to the time samples in the estimation window, x_k and u_k denote the estimated states and inputs at these samples, x_N is the estimate of the current state, and x_0 is the estimate at the beginning of the estimation window, i.e. N samples in the past. $\bar{y}_k$ and $\bar{y}_N$ denote actual measurements, h and h_N are measurement models. S_{AC}, W_k and W_N are weighting matrices. The constraint (5b) is the (nonlinear) system model,[3] the constraints (5c) and (5d) place bounds (box constraints) on the states and inputs.

x_{AC} is the best available estimate of x_0 before the current sample, e.g. the estimate of x_1 from the previous sample. The first term in the objective function (5a) penalizes any deviation in the estimated x_0 from x_{AC}, as x_{AC} and S_{AC} contain all information obtained before the estimation horizon. This is commonly referred to as the *arrival cost* (AC). The weighting matrices may change between each sample, and indeed, S_{AC} is commonly updated by Kalman Filter-based updates after each new measurement (Rao et al., 2003). The other two terms in the objective function penalize deviation between actual measurements and estimated measurements modeled by h and h_N, thus the estimator will seek to find estimates such that the behavior of the model corresponds to the actual dynamics observed.

Even though the inputs typically are known (measured) variables, they are also decision variables in the MHE formulation. This means that the estimator is not restricted to use the *exact* measurements of the inputs when fitting the model to the measurements, and a noise filtering effect is thus introduced. On the other hand, deviations in the estimates from the measurements are penalized by the weights in W_k, and reliable measurements should have large weights.

Further details regarding ACADO Code Generation and the MHE problem formulation can be found in Houska et al. (2009–2013).

3.3 MHE Formulation for the ESP-lifted Well

A MHE problem for the considered system is implemented in C++ as an Optimal Control Problem (OCP) using

[3] (5b) describes a discrete-time system model. However, the current version of ACADO Code Generation tool only supports a continuous-time formulation of the system model; discretization is automatically performed by ACADO.

Copyright © 2015, IFAC

Table 5. MHE settings

N	15
N_i	5
T_s	1 second
Integrator type	Explicit Runge-Kutta 4
Discretization type	Multiple shooting

ACADO syntax (cf. Houska et al. (2009–2013)), formulated as (5). The model given by (1)-(2) is also written in this syntax and given as constraint (5b) in the OCP.

The parameters μ and PI are added as states with differential equations:

$$\dot{\mu} = 0 \tag{6a}$$

$$\dot{\text{PI}} = 0 \tag{6b}$$

The measured disturbance p_m is treated as an input. The state and input vectors are thus given by:

$$x = [p_{bh},\, p_{wh},\, q,\, \mu,\, \text{PI}]^T \tag{7a}$$

$$u = [f,\, z,\, p_m]^T \tag{7b}$$

The estimated measurement function h is given by:

$$h = [I,\, p_{p,in},\, \Delta p_p,\, f,\, z,\, p_m,\, p_{wh}]^T \tag{8}$$

and is implemented using the model (1)-(2) and (3). [4] As h_N may not depend on any inputs in ACADO, it is not used.

The constraints (5c) and (5d) on the states and inputs, respectively, are derived from physical considerations and system knowledge, and are given by:

$$35 \leq \ f \ \leq 65 \quad [\text{Hz}] \tag{9a}$$

$$0 \leq \ z \ \leq 100 \quad [\%] \tag{9b}$$

$$1 \leq p_m \leq 50 \quad [\text{bar}] \tag{9c}$$

$$1 \leq p_{wh} \leq 60 \quad [\text{bar}] \tag{9d}$$

$$1 \leq p_{bh} \leq p_r \quad [\text{bar}] \tag{9e}$$

$$0 \leq \ q \qquad [\text{m}^3/\text{s}] \tag{9f}$$

$$0.1 \leq \ \mu \ \leq 500 \quad [\text{cP}] \tag{9g}$$

Constraints on the inputs are included to provide better estimates, e.g. the choke will never be estimated to be more than 100 % open.

3.4 Settings and Weighting

There are a lot of settings that may affect the performance of the MHE, including the length N of the estimation horizon, number of integrator steps per sampling interval N_i, integrator type and discretization type. The settings used in the simulations are given in table 5.

The weighting matrix W_k is the main tuning parameter in the estimator. In general, the weights should be chosen based on how much the measurements and the measurement models can be trusted. A noisier measurement or a less accurate model should have a smaller weight. The weights W_k used in this paper are given by

$$W_k = \texttt{diag}(1,\, 1,\, 0.67,\, 33.3,\, 10,\, 4,\, 3.33),\ \forall\, k \tag{10}$$

[4] While SI units are used in the model and simulations, the pressures in the measurement function are given in [bar], and the choke opening in [%], for a better relative scaling of the variables.

Table 6. Standard deviation of measurement noise

Measurement	I	$p_{p,in}$	Δp_p	f	z	p_m	p_{wh}
Std. dev. (σ)	0.02	0.02	0.02	0.005	0.001	0.01	0.01

These are mainly derived from the inverse of the standard deviation of the measurement noise for each measurement, given in table 6, and the inputs are weighted more than the modeled measurements. The weights are also scaled according to the typical range of each variable.

While ACADO includes functionality for Kalman Filter-based updates of the arrival cost weighting matrix S_{AC} (see section 3.1), a constant S_{AC} is used in the simulations. This introduces more degrees of freedom when tuning the estimator. The (original) model states are weighted quite evenly in S_{AC}, but the parameters μ and especially PI have large weights. PI is assumed to be constant, and a large arrival cost ensures that this parameter does not change too fast in the estimation. The arrival cost used is given by

$$S_{AC} = \texttt{diag}(1\,\text{e}{-10},\, 2\,\text{e}{-10},\, 5\,\text{e}\,7,\, 1\,\text{e}\,2,\, 5\,\text{e}\,23) \tag{11}$$

The state vector (7a) is given in SI units, and the arrival cost is scaled accordingly.

4. SIMULATION RESULTS

Simulation results of the implemented MHE are presented in this section.

4.1 Test Scenario

Data from a simulation scenario presented in Binder et al. (2014), where an MPC was implemented for the system, is used as a test scenario for the MHE. [5] The scenario is modified to include a varying viscosity of the produced fluid. The viscosity can change relatively fast due to phenomena like phase inversion, where the flow transitions from oil being present as droplets in a water continuous flow, to water being present in an oil continuous flow, or vice versa (Piela et al., 2008). In the model used in the simulations, a change in the viscosity of the produced fluid affects the whole well instantaneously, while in a real well, a change in the viscosity would only propagate with the speed of the flow in the well. The well dynamics would thus be a lot slower as e.g. the friction in the well would change slowly. In the simulations, we have tested the MHE in an extreme (although somewhat unrealistic) scenario to challenge the estimator and evaluate its performance in extreme conditions.

4.2 Measurement Noise

The MHE is tested with measurement noise. Each measurement is generated using

$$y = (1 + n) \cdot y_{real} \tag{12}$$

where n is a noise signal with normal distribution. The standard deviation of the measurement noise for each measurement is given in table 6.

[5] The model used to generate the simulation data is identical to the model used in the MHE, except that the MHE model assumes a constant density ρ, and that they are discretized differently.

Copyright © 2015, IFAC

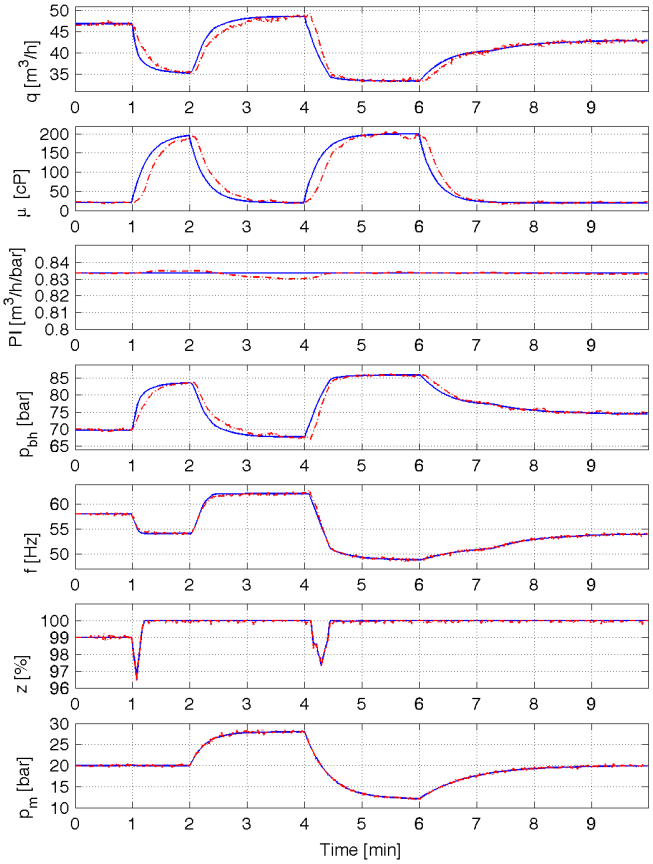

Fig. 3. Estimation results

Table 7. Mean estimation error [%]

Time	1-2	2-3	3-4	4-5	5-6	6-7	7-8	8-9
q	3.5	-3.9	-0.8	3.8	0.3	-2.1	0.2	-0.1
μ	-24.5	43.7	9.5	-24.2	-1.7	29.9	-3.3	0.4
PI	0.1	0.0	-0.3	-0.1	0.0	0.0	0.0	-0.0
p_{bh}	-1.7	2.6	0.4	-2.2	-0.1	1.0	-0.1	0.1

4.3 Estimation Results

MHE estimation results are presented in Fig. 3. The real data is shown as solid blue lines, the estimates are shown as dash-dotted red lines. As can be seen, all estimates are quite accurate, without any steady-state offset, though there is a small lag in the estimates. The estimator does not have any information about the dynamics of the parameter μ, which changes very fast in this scenario, while $\dot{\mu} = 0$ is assumed in the estimator model. This means that the estimator needs to use feedback from the measurements to make correction for this, and this needs some time in order not to amplify measurement noise too much. This error propagates to the other states, as the parameter μ is an essential parameter in the system model.

In table 7, the average estimation error (in percent) is calculated for each minute of the simulation. Due to the lag in the estimates, there are large relative errors during the transients, especially for the estimates of viscosity μ. The estimates at steady-state are quite accurate, see e.g. the last time interval in the table, from 8 to 9 minutes in the simulation.

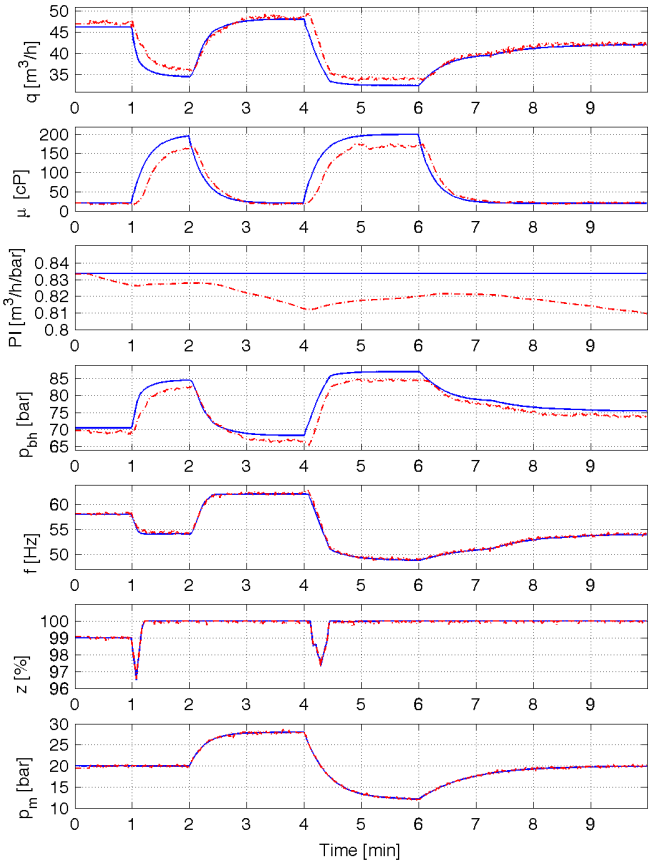

Fig. 4. Estimation results with increased density

Table 8. Mean estimation error with increased density [%]

Time	1-2	2-3	3-4	4-5	5-6	6-7	7-8	8-9
q	7.2	-0.8	0.9	7.0	4.7	0.6	1.0	1.2
μ	-34.3	18.4	-9.7	-33.7	-15.3	22.2	11.0	-1.0
PI	-0.7	-0.9	-1.9	-2.2	-1.8	-1.5	-1.6	-2.1
p_{bh}	-4.1	-0.3	-2.4	-5.0	-2.9	-1.3	-1.7	-2.2

4.4 Parameter Sensitivity

Although many parameters in the model are assumed to be known and constant, some parameters may be inaccurate or varying. E.g. the fluid density ρ may change in the period between the times fluid samples are taken, and thus may be inaccurate. To investigate how such model inaccuracies may affect the estimations, a simulation with an increased fluid density is performed. ρ is set to 1000 kg/m^3 in the simulator, while it is kept at 950 kg/m^3 in the estimator model. The results are shown in Fig. 4 and table 8. The estimates are still quite good, though the highest viscosity levels are not estimated very accurately, and the estimates of the flow rate are thus a bit too high, e.g. in the interval between 5 and 6 minutes. The estimates of PI are also less accurate. Nevertheless, this shows that the estimator is quite robust to unknown errors in the model parameters.

4.5 Computation Time

As mentioned in section 3.1, the nonlinear MHE problem is solved in two phases. A feedback phase is run for each

Copyright © 2015, IFAC

Table 9. MHE computation time in [μs]

Mode	Preparation		Feedback		Total	
	Avg.	Worst	Avg.	Worst	Avg.	Worst
Original	300	430	496	833	796	1 263
Increased ρ	300	479	490	1 079	790	1 467

new measurement, and a preparation phase is run after the estimate is ready, to prepare for the next measurement. The computation times of the MHE solver on a computer running OS X 10.9, with a 2.6 GHz Intel Core i7 processor and 16 BG of RAM, are presented in table 9. As can be seen in the table, the solver is very fast, and the MHE problem is solved in less than a millisecond on average. The worst-case computation time is less than 1.5 milliseconds.

5. CONCLUSIONS

In this paper, a Moving Horizon Estimator was successfully implemented for a well with an Electric Submersible Pump. The implemented estimator was able to estimate the flow rate and the productivity index of the well, and the viscosity of the produced fluid. ACADO was used to implement the estimator, and proved to be a capable software package, providing a fast and efficient solver for the MHE problem. As the solver was very fast, the estimator may also be feasible to implement on industrial embedded hardware, though this was not investigated in this paper.

REFERENCES

Aamo, O.M., Eikrem, G.O., Siahaan, H.B., and Foss, B.A. (2005). Observer design for multiphase flow in vertical pipes with gas-lift—-theory and experiments. *Journal of Process Control*, 247–257.

Beall, R.Q., Sheth, K.K., and Olsen, H. (2011). An integrated solution enabling allocation of heavy oil in the peregrino field. In *Offshore Technology Conference*. Houston, TX, USA.

Binder, B.J.T., Kufoalor, D.K.M., Pavlov, A., and Johansen, T.A. (2014). Embedded Model Predictive Control for an Electric Submersible Pump on a Programmable Logic Controller. In *Proc. 2014 IEEE Conference on Control Applications (CCA)*.

Bloemen, H., Belfroid, S., Sturm, W., and Verhelst, F. (2004). Soft sensing for gas-lift wells. In *SPE Annu. Tech. Conf. and Exhibition*. Houston, TX, USA.

Diehl, M., Bock, H.G., Schlöder, J.P., Findeisen, R., Nagy, Z., and Allgöwer, F. (2002). Real-time optimization and nonlinear model predictive control of processes governed by differential-algebraic equations. *Journal of Process Control*, 12(4), 577–585.

Eikrem, G.O., Imsland, L.S., and Foss, B. (2004). Stabilization of gas lifted wells based on state estimation. In *International Symposium on Advanced Control of Chemical Processes*.

Ferreau, H., Kirches, C., Potschka, A., Bock, H., and Diehl, M. (2014). qpOASES: A parametric active-set algorithm for quadratic programming. *Mathematical Programming Computation*. (in print).

Hasan, A. and Imsland, L. (2014). Moving horizon estimation in managed pressure drilling using distributed models. In *Proc. 2014 IEEE Conference on Control Applications (CCA)*, 605–610.

HI (1969). *Determination of Pump Performance when Handling Viscous Liquid*. Hydraulic Institute Standards, 20th edition.

Houska, B., Ferreau, H., and Diehl, M. (2011). ACADO Toolkit – An Open Source Framework for Automatic Control and Dynamic Optimization. *Optimal Control Applications and Methods*, 32(3), 298–312.

Houska, B., Ferreau, H., Vukov, M., and Quirynen, R. (2009–2013). ACADO Toolkit User's Manual. http://www.acadotoolkit.org.

Julier, S.J. and Uhlmann, J.K. (2004). Unscented filtering and nonlinear estimation. *Proceedings of the IEEE*, 92(3), 401–422.

Kaasa, G.O., Stamnes, Ø.N., Aamo, O.M., and Imsland, L.S. (2012). Simplified hydraulics model used for intelligent estimation of downhole pressure for a managed-pressure-drilling control system. *SPE Drilling and Completion*, 27(1), 127–138.

Kühl, P., Diehl, M., Kraus, T., Schlöder, J.P., and Bock, H.G. (2011). A real-time algorithm for moving horizon state and parameter estimation. *Computers & Chemical Engineering*, 35(1), 71–83.

Nikoofard, A., Johansen, T.A., and Kaasa, G.O. (2014). Design and comparison of adaptive estimators for underbalanced drilling. In *Proc. 2014 American Control Conference (ACC)*. Portland, OR, USA.

Olsen, H., Sheth, K., Pessoa, R., Rutter, R., and Crossley, A. (2012). Successful production allocation through esp performance in peregrino field. In *SPE Latin American and Caribbean Petroleum Engineering Conference*. Mexico City, Mexico.

Paasche, M., Johansen, T.A., and Imsland, L.S. (2011). Regularized and adaptive nonlinear moving horizon estimation of bottomhole pressure during oil well drilling. In *Proc. 2011 IFAC World Congress*. Milan, Italy.

Pavlov, A. and Alstad, V. (2010). Modelling, simulation and automatic control of ESP lifted wells. Statoil internal report.

Pavlov, A., Krishnamoorthy, D., Fjalestad, K., Aske, E., and Fredriksen, M. (2014). Modelling and model predictive control of oil wells with electric submersible pumps. In *Proc. 2014 IEEE Conference on Control Applications (CCA)*.

Piela, K., Delfos, R., Ooms, G., Westerweel, J., and Oliemans, R. (2008). On the phase inversion process in an oil–water pipe flow. *Int. J. Multiphase Flow*.

Rao, C.V., Rawlings, J.B., and Mayne, D.Q. (2003). Constrained state estimation for nonlinear discrete-time systems: Stability and moving horizon approximations. *IEEE Trans. Autom. Control*.

Siahaan, H.B. and Nygaard, G. (2008). On modeling and observer design of fluid flow dynamics for petroleum drilling operations. In *Proc. 47th IEEE Conf. Decision and Control (CDC08)*. Cancun, Mexico.

Takacs, G. (2009). *Electrical Submersible Pumps Manual: Design, Operations, and Maintenance*. Gulf Equipment Guides. Gulf Professional Publishing, 1 edition.

Varón, M.P., Biazussi, J.L., Bannwart, A.C., Verde, W.M., and Sassim, N. (2013). Study of an electrical submersible pump (esp) as flow meter. In *SPE Artificial Lift Conference - Americas*. Cartagena, Colombia.

Copyright © 2015, IFAC